



**HAL**  
open science

## **$J/\Psi\psi'$ and Drell-Yan production in pp and pd interactions at 450 GeV/c**

M C. Abreu, B. Alessandro, A. Baldit, C. Barriere, M. Bedjidian, P. Bordalo, J. Castor, T. Chambon, B. Chaurand, E. Chiavassa, et al.

► **To cite this version:**

M C. Abreu, B. Alessandro, A. Baldit, C. Barriere, M. Bedjidian, et al..  $J/\Psi\psi'$  and Drell-Yan production in pp and pd interactions at 450 GeV/c. Physics Letters B, 1998, 438, pp.35-40. 10.1016/S0370-2693(98)01014-4 . in2p3-00005052

**HAL Id: in2p3-00005052**

**<https://hal.in2p3.fr/in2p3-00005052>**

Submitted on 5 Nov 2006

**HAL** is a multi-disciplinary open access archive for the deposit and dissemination of scientific research documents, whether they are published or not. The documents may come from teaching and research institutions in France or abroad, or from public or private research centers.

L'archive ouverte pluridisciplinaire **HAL**, est destinée au dépôt et à la diffusion de documents scientifiques de niveau recherche, publiés ou non, émanant des établissements d'enseignement et de recherche français ou étrangers, des laboratoires publics ou privés.

# $J/\psi$ , $\psi'$ and Drell-Yan production in pp and pd interactions at 450 GeV/c

M.C. Abreu<sup>1,a)</sup>, B. Alessandro<sup>2)</sup>, A. Baldit<sup>3)</sup>, C. Barrière<sup>3)</sup>, M. Bedjidian<sup>4)</sup>,  
P. Bordalo<sup>1,b)</sup>, J. Castor<sup>3)</sup>, T. Chambon<sup>3)</sup>, B. Chaurand<sup>5)</sup>, E. Chiavassa<sup>2,c)</sup>,  
D. Contardo<sup>4)</sup>, G. Dellacasa<sup>2,d)</sup>, N. De Marco<sup>2)</sup>, E. Descroix<sup>4,e)</sup>, A. Devaux<sup>3)</sup>,  
O. Drapier<sup>4)</sup>, B. Espagnon<sup>3)</sup>, J. Fargeix<sup>3)</sup>, F. Fleuret<sup>5)</sup>, R. Ferreira<sup>1)</sup>, P. Force<sup>3)</sup>,  
J. Gago<sup>1,b)</sup>, M. Gallio<sup>2,c)</sup>, C. Gerschel<sup>6)</sup>, P. Giubellino<sup>2)</sup>, P. Gorodetzky<sup>7,g)</sup>,  
J.Y. Grossiord<sup>4)</sup>, P. Guaita<sup>2)</sup>, A. Guichard<sup>4)</sup>, R. Haroutunian<sup>4)</sup>, D. Jouan<sup>6)</sup>,  
L. Kluberg<sup>5)</sup>, G. Lандаud<sup>3)</sup>, D. Lazic<sup>7)</sup>, C. Lourenço<sup>1,f)</sup>, R. Mandry<sup>4)</sup>,  
A. Marzari-Chiesa<sup>2,c)</sup>, M. Maserà<sup>2,c)</sup>, M. Monteno<sup>2)</sup>, A. Musso<sup>2)</sup>,  
F. Ohlsson-Malek<sup>4,h)</sup>, A. Piccotti<sup>2)</sup>, J.R. Pizzi<sup>4)</sup>, C. Racca<sup>7)</sup>, L. Ramello<sup>2,d)</sup>,  
S. Ramos<sup>1,b)</sup>, L. Riccati<sup>2)</sup>, A. Romana<sup>5)</sup>, P. Saturnini<sup>3)</sup>, E. Scomparin<sup>2,f)</sup>,  
S. Silva<sup>1)</sup>, P. Sonderegger<sup>8,b)</sup>, X. Tarrago<sup>6)</sup>, J. Varela<sup>1,b,f)</sup>, F. Vazeille<sup>3)</sup>,  
E. Vercellin<sup>2,c)</sup>

## *NA51 Collaboration*

$J/\psi$  and  $\psi'$  production cross-sections are measured in pp and pd collisions at 450 GeV/c at the CERN-SPS. The Drell-Yan cross section for muon pairs in the mass range [4.3 – 8.0] GeV/c<sup>2</sup> is also determined in the same experiment.

- 
- 1) LIP, Av. Elias Garcia 14, P-1000 Lisbon, Portugal  
2) Università di Torino e INFN, Via Pietro Giuria 1, I-10125 Torino, Italia  
3) LPC Clermont-Ferrand, IN2P3-CNRS and Université Blaise Pascal, F-63177 Aubière Cedex, France  
4) IPN Lyon, IN2P3-CNRS and Université Claude Bernard, F-69622 Villeurbanne Cedex, France  
5) LPNHE, Ecole Polytechnique, IN2P3-CNRS, F-91128 Palaiseau Cedex, France  
6) IPN, IN2P3-CNRS and Université de Paris-Sud, F-91406 Orsay Cedex, France  
7) IRes, IN2P3-CNRS and Université Louis Pasteur, F-67037 Strasbourg Cedex, France  
8) CERN, CH-1211 Geneva 23, Switzerland  
a) Also at FCUL, Universidade de Lisboa, Lisbon, Portugal  
b) Also at IST, Universidade Técnica de Lisboa, Lisbon, Portugal  
c) Dipartimento di Fisica Sperimentale  
d) Dipartimento di Scienze e tecnologie Avanzate, II Facoltà di Scienze, Alessandria  
e) Now at Université Jean Monnet, Saint-Etienne, France  
f) Now at CERN, Geneva, Switzerland  
g) Now at PCC Collège de France, Paris, France  
h) Now at ISN, Grenoble, France

# 1 Introduction

Experiment NA51 was performed in 1992 in order to check the apparent violation of the Gottfried sum rule [1] and led to a clear indication of isospin symmetry violation in the light quark sea of the nucleon [2, 3]. This result was obtained by studying, in pp and pd collisions at 450 GeV/c incident momentum, the production of Drell-Yan pairs with an invariant mass above 4.3 GeV/c<sup>2</sup>. The same high statistics sample of data is used here to measure absolute cross sections of J/ψ and ψ' vector mesons as well as of the high mass Drell-Yan continuum.

# 2 Apparatus and data

The NA51 experiment has been described in ref. [2]. It makes use of the primary 450 GeV/c proton beam from the CERN-SPS at an average intensity of 10<sup>9</sup> protons per second. Muon pairs are detected with the NA10 spectrometer [4] especially designed for high intensity incident beams. Muons are tracked by 8 multiwire proportional chambers and bent, for momentum determination, in the magnetic field of an air-core toroidal magnet ( $\int Bdl \approx 1.2$  Tm at a radius of 75 cm). They are filtered in a 4 m long carbon and 0.8 m long iron absorber and trigger the experiment by hitting 4 hodoscopes of plastic scintillator slabs. More details can be found in ref. [4].

The target system is made of three identical vessels, respectively empty (10<sup>-2</sup> torr) and filled with liquid hydrogen and deuterium. The targets are 120 cm long and 3 cm in diameter which, given the beam dimensions, ensures a 100 % targetting efficiency. The empty target is used to subtract the contribution of reactions in the vessel windows made of 30 μm of stainless steel and of 76 μm of aluminium. The targets are mounted on a remote control system which allows to change periodically the target exposed to the beam.

The numbers of recorded events are shown in table 1. They include a contribution

Target	H2	D2	empty
total number of events	1.0 10 <sup>7</sup>	1.3 10 <sup>7</sup>	7 10 <sup>5</sup>
events with 2.7 < M <sub>μμ</sub> < 3.5 GeV/c <sup>2</sup>	434623	450878	2637
events with M <sub>μμ</sub> > 4.3 GeV/c <sup>2</sup>	2763	3007	16

Table 1: Total number of recorded events as well as selected events in the J/ψ and Drell-Yan mass regions for each target.

of pairs originating from the decay of pions and kaons. This background can be estimated from the number of like-sign pairs according to the relation

$$N_{bg} = 2R_{bg} \times \sqrt{N^{++} \times N^{--}}$$

where  $N_{bg}$  is the number of opposite-sign background muon pairs and  $N^{++}$  ( $N^{--}$ )

are the numbers of  $\mu^+\mu^+$  ( $\mu^-\mu^-$ ) muon pairs. It can be shown that the estimate is valid provided that the probability to detect a muon in the apparatus is independent of its charge. We thus apply a fiducial cut which rejects any muon pair where at least one of the muons would have been out of acceptance in a reversal of the sign of the magnetic field. The value of  $R_{bg}$  depends on the number of accepted positive and negative muons. It is expected to be equal to 1 if the parent  $\pi$  and K mesons are uncorrelated and if their multiplicity distribution is poissonian. In the case of low multiplicity events like those produced in pp and pd collisions, the  $R_{bg}$  factor may be higher than 1 because of correlations due to charge conservation constraints. However, in this experiment, due to the high beam intensity, the background is essentially produced by uncorrelated pairs originating from two different interactions<sup>1</sup>. It is thus justified to take  $R_{bg} = 1$ . In order to check this assumption, we have also fit the data with  $R_{bg}$  as a free parameter. The best  $\chi^2$  is obtained for  $R_{bg} = 1$ . The signal is then defined by  $N_{signal} = N^{+-} - N_{bg}$  where  $N^{+-}$  is the number of pairs with opposite sign muons. More details about this background subtraction can be found in ref. [5]. The number of events surviving all the selection cuts are shown in table 1.

The invariant mass resolution of the muon pairs ( $\sigma = 175 \text{ MeV}/c^2$  for the  $J/\psi$ ) is dominated by multiple scattering in the absorber. It suffers from the length of the target which provides a loose constraint on the vertex  $z$  coordinate.

### 3 Data analysis

The analysis is restricted to the kinematical domain where the differential acceptance is higher than 1 %, i.e. for  $-0.4 < y_{cm} < 0.6$  and  $|\cos(\theta_{CS})| < 0.5$  where  $y_{cm}$  is the c.m.s rapidity and  $\cos(\theta_{CS})$  is the polar decay angle of the muons in the Collins-Soper reference frame. Invariant mass spectra are shown in figures 1 and 2 for pp and pd collisions, respectively. For invariant masses above  $1.5 \text{ GeV}/c^2$ , opposite sign pairs originate from five mechanisms: the background, defined as explained above,  $J/\psi$ ,  $\psi'$ , Drell-Yan pairs and muon pairs originating from the semi-leptonic decay of  $D$  and  $\bar{D}$  mesons. For the four signal sources, muon pairs are generated with a Monte-Carlo simulation and propagated through the detector in order to get a sample of simulated events which undergo reconstruction rules and selection cuts identical to those of the experimental sample. For the  $J/\psi$  and  $\psi'$  events, we use a gaussian rapidity distribution with an initial r.m.s. value  $\sigma = 0.6$  and a uniform  $\cos(\theta_{CS})$  distribution. The transverse momentum is generated with the function  $K_1(\frac{M_T}{T})$  where  $K_1$  is the modified Bessel function and  $T = 236 \text{ MeV}$  is the initial value. The parameter values are tuned in successive iterations until they provide a good reproduction of the measured  $p_T$  and  $y$  distributions. The Drell-Yan mass distribution is calculated at leading order using the MRS A (LQ) parametrization of the parton distribution functions [6], as provided

---

<sup>1</sup>This is confirmed by the quadratic evolution of the background with the beam intensity.

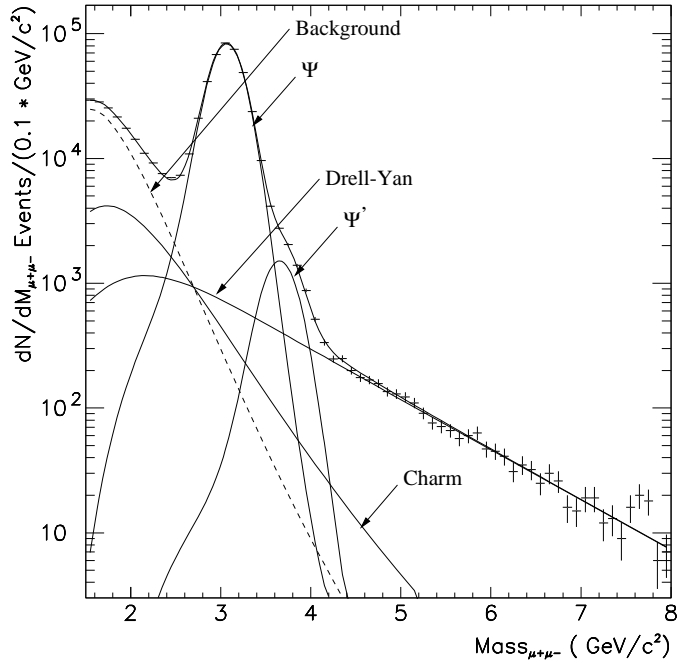


Figure 1: Invariant mass spectrum of  $\mu^+\mu^-$  pairs for pp collisions. Results from the fit are also shown.

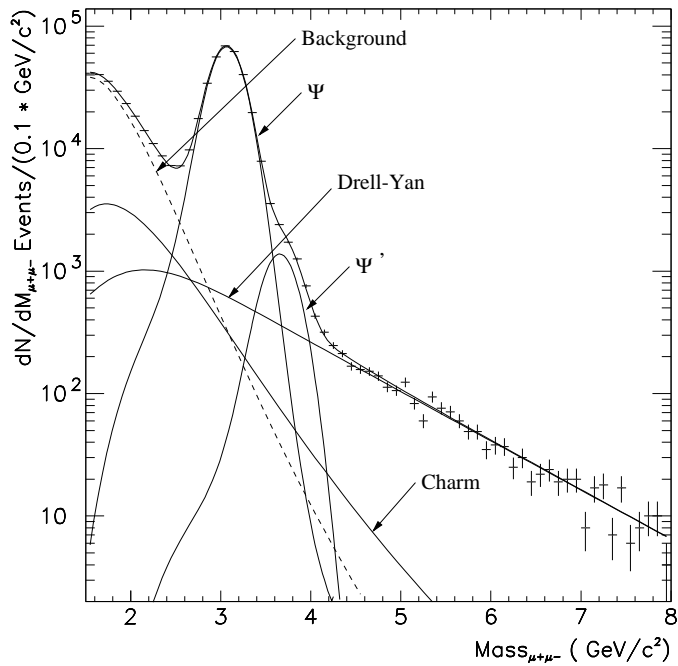


Figure 2: Invariant mass spectrum of  $\mu^+\mu^-$  pairs for pd collisions. Results from the fit are also shown.

by the PDFLIB package [7], with a  $p_T$ -dependence similar to that of  $J/\psi$ . Since the acceptance of the spectrometer is basically flat as a function of  $p_T$  in the high mass region, the accepted mass distribution is rather insensitive to the  $p_T$ -distribution used in the event generation. The MRS A (LQ) parametrization of the parton distribution function accounts for the isospin asymmetry in the light sea quark of the nucleon [2] which affects significantly the pp and pd Drell-Yan cross sections. To the precision of the present experiments, the leading order calculation reproduces well the shape of the Drell-Yan spectrum. Higher order terms appear only as a multiplicative factor  $K$  which is independent of the invariant mass [8, 9]. The  $D\bar{D}$  events are generated with a 0.8 GeV width gaussian primordial  $k_T$  distribution. The quark charm mass is assumed to be 1.5 GeV.

The resulting shapes of the dimuon mass distributions, obtained for the three simulated processes, are parametrized by empirical functional forms. The shape of the reconstructed  $J/\psi$  resonance is described by a pseudo gaussian function:

$$\frac{dN}{dM} \propto e^{-\frac{(M-\mu)^2}{2(\sigma_0\varphi(M))^2}}$$

where  $\sigma_0\varphi(M)$  [10] is a mass dependent width determined to reproduce the shape of the resonance. A similar shape is used for the  $\psi'$ . The corresponding parameters  $\mu'$  and  $\sigma'_0$  are related to  $\mu$  and  $\sigma_0$  according to the following relations:  $\mu' = \mu + \Delta M$  where  $\Delta M$  is the mass difference between  $J/\psi$  and  $\psi'$  resonances as given by the Particle Data Group [11] and  $\sigma'_0 = \sigma_0 \frac{\sigma'_{0sim}}{\sigma_{0sim}}$  where  $\sigma'_{0sim}$  and  $\sigma_{0sim}$  are the values that fit the simulated histograms. The shape of the Drell-Yan component is well reproduced by the superposition of two exponential functions:

$$\frac{dN}{dM} \propto e^{-P_1 M} + P_2 \times e^{-P_3 M}.$$

Finally the shape of the  $D\bar{D}$  component is parametrized as:

$$\frac{dN}{dM} \propto e^{-C_1 M} - C_2 \times e^{-C_3(M-C_4)^3}.$$

The global fit to the signal mass spectrum makes use of the maximum likelihood method and has six free parameters, which are the above mentioned  $\mu$  and  $\sigma_0$  values, the  $J/\psi$  and  $D\bar{D}$  normalizations  $N_\psi$  and  $N_{D\bar{D}}$  and the ratios  $N_{\psi'}/N_\psi$  and  $N_\psi/N_{DY}$  where  $N_\psi$ ,  $N_{\psi'}$  and  $N_{DY}$  are the relative numbers of  $J/\psi$ ,  $\psi'$  and Drell-Yan events. The results of the fits are shown in figures 1 and 2.

## 4 Results

In order to determine the absolute cross section of the different processes, we need the luminosity and all the experimental efficiencies. The beam intensity is obtained from three independent multifoil ionization chambers filled with argon. Their linearity was checked at low intensity with scintillating counters and then monitored at high intensity with three telescopes, pointing at 90° to the target,

which count the number of produced particles in their small solid angle. These telescopes are made of three scintillators each and are shielded against neutrons by blocks of paraffin. Their low counting rate guarantees full efficiency even at the high nominal intensity of the experiment.

Acceptances, efficiencies and numerical constants used for the calculation of the cross sections are listed in table 2. To evaluate the effect of the event multiplicity on the track reconstruction efficiency, particularly important at high intensity, we have simulated  $J/\psi$  events and, taking into account the chamber inefficiency, we have merged them with high multiplicity experimental events. We could thus get a severe check of the reconstruction procedure. The ratio between the efficiency corrected number of  $J/\psi$ 's and the beam intensity is found constant for all the collected runs within an accuracy of 1%. Finally we have also indicated in the

	H2	D2
Calibration of the beam detectors	$100 + 0 - 4\%$	$100 + 0 - 4\%$
Trigger efficiency	$94 \pm 5\%$	$94 \pm 5\%$
$\rho L_{eff} (g / cm^2)$	$7.82 \pm 0.04$	$16.36 \pm 0.09$
$J/\psi$ acceptance	$13.19 \pm 0.07\%$	$13.17 \pm 0.07\%$
$\psi'$ acceptance	$15.89 \pm 0.07\%$	$15.75 \pm 0.07\%$
Drell-Yan acceptance ( $4.3 < M_{\mu\mu} < 8 \text{ GeV}/c^2$ )	$18.18 \pm 0.07\%$	$18.42 \pm 0.07\%$

Table 2: Acceptances, efficiencies and numerical constants used for the calculation of the cross sections.

table the effective length of each target  $\rho L_{eff}$  where the uncertainty is due to the uncertainty on the density  $\rho$ <sup>2</sup>. The total systematic error on the absolute normalization amounts to 7 %. The results are shown in table 3 and take into account a systematic error due to the fit procedure. It should be noted that the uncertainties on the calibration and on the efficiency should be ignored when comparing pp and pd results as they are the same for both data sets. The resulting reduced systematic errors are also given in parentheses in table 3.

## 5 Discussion

As can be seen from table 3, the ratios  $B'\sigma_{\psi'}/B\sigma_{\psi}$  are similar for both targets. This ratio has indeed been found to be constant whatever the target mass number and the projectile energy [12, 13, 14] within the large uncertainties of the measurements. We can also compare the cross sections obtained in the two reactions for the different processes. Since  $J/\psi$  and  $\psi'$  are produced mostly by gluon fusion at

---

<sup>2</sup>The effective length is calculated as  $\rho L_{eff} = \rho\lambda_I(1 - \exp(-L/\lambda_I))$  where L is the thickness of the target and  $\lambda_I$  its interaction length.

Target	H2	D2
$N_\psi$	$301236 \pm 601$	$312204 \pm 630$
$N_{\psi'}$	$5705 \pm 127$	$6219 \pm 131$
$N_{DY}$	$1910 \pm 44$	$2120 \pm 46$
$B\sigma_\psi$ (nb)	$5.50 \pm 0.01 \pm 0.36(0.06)$	$11.32 \pm 0.03 \pm 0.75(0.13)$
$B'\sigma_{\psi'}$ (nb)	$0.086 \pm 0.002 \pm 0.006(0.003)$	$0.188 \pm 0.004 \pm 0.015(0.006)$
$\sigma_{DY}$ (pb)	$25.3 \pm 0.6 \pm 1.8(0.5)$	$55.0 \pm 1.2 \pm 3.9(1.2)$
$B'\sigma_{\psi'}/B\sigma_\psi$ (%)	$1.60 \pm 0.04 \pm 0.02$	$1.72 \pm 0.04 \pm 0.025$
$B\sigma_\psi/\sigma_{DY}$	$54.7 \pm 1.0 \pm 1.3$	$53.8 \pm 1.0 \pm 0.5$

Table 3: Numbers of  $J/\psi$ ,  $\psi'$  and Drell-Yan events in the mass range [4.3–8.0]  $\text{GeV}/c^2$  as well as the corresponding cross sections. B and B' are the branching ratios of the decay of  $J/\psi$  and  $\psi'$  resonances into two muons. Ratios of cross sections are also given. In the case of the ratio  $B\sigma_\psi/\sigma_{DY}$ , Drell-Yan pairs are taken in the mass range [2.9–4.5]  $\text{GeV}/c^2$  in order to allow the comparison with other data from the NA38 experiment. Finally, the numbers given in parenthesis correspond to the fraction of systematic error which has to be taken into account in the comparison of the two targets.

these energies, no isospin effect is expected for the deuterium target. However, for Drell-Yan events, the deuterium cross section is not expected to be simply twice the value obtained for hydrogen because the elementary Drell-Yan pp and pn cross sections are not equal. For comparison purposes, we treat deuterium as if it was made of two protons and rescale the cross section according to

$$\sigma(pd)_{DY}^{corr} = \sigma(pd)_{DY}^{meas} \times \frac{2 \times \sigma(pp)_{DY}^{MRS}}{\sigma(pd)_{DY}^{MRS}}$$

where  $\sigma(pp)_{DY}^{MRS}$  and  $\sigma(pd)_{DY}^{MRS}$  are the lowest order cross sections of pp and pd collisions. The correction factor is 0.91. In table 4, we have displayed the cross sections per nucleon, i.e. the cross sections divided by the mass number of the target. For the two reactions, the different cross sections are rather close with a  $\simeq 1.5 \sigma$  difference for  $J/\psi$  and  $\psi'$ . The similarity of  $J/\psi$  and  $\psi'$  cross sections may seem curious given the mass number dependence of the charmonia cross section measured with heavier targets. If we apply the scaling law obtained,  $A^\alpha$  with  $\alpha \simeq 0.91$ , to the deuterium target, the deuterium cross section should be 6% smaller than the hydrogen one. This is not the case. It can be understood because deuterium is a weakly bound nucleus and the proton and the neutron can be considered as if they were quasi independent. This has also been observed for the inelastic cross section in pA collisions [15].

We can finally compare the  $J/\psi$  pp cross section to the cross section obtained previously by experiment NA3 [16] at 200  $\text{GeV}/c$  incident momentum, i.e.

$B\sigma_\psi = 3.6 \pm 0.6$  nb. The NA3 cross section has to be rescaled in order to take



Target	H2	D2
$B\sigma_\psi/A$ (nb)	$5.50 \pm 0.06$	$5.66 \pm 0.07$
$B'\sigma_{\psi'}/A$ (nb)	$0.086 \pm 0.004$	$0.094 \pm 0.004$
$\sigma_{DY}^{corr}/A$ (pb)	$25.3 \pm 0.8$	$25.0 \pm 0.8$

Table 4: Cross sections per nucleon of  $J/\psi$ ,  $\psi'$  and Drell-Yan events in the mass range [4.3–8.0] GeV/ $c^2$ , i.e. cross sections divided by the atomic mass  $A$  of the target. An isospin correction factor of 0.91 is introduced for the Drell-Yan cross section of the deuterium target which is treated as if it was made of two protons. The systematic errors which are considered here do not include the part related to the calibration of the beam detectors and to the trigger efficiency, which are the same for both targets.

into account the difference in c.m.s. energy and kinematical domain from NA51: for NA3, the whole forward hemisphere has been considered while for NA51 the  $x_F$  domain is restricted to  $[-0.18, +0.14]$ . The correction factor is  $2 \times (0.437 \pm 0.087) = 0.86 \pm 0.17$  which is explained in the following way: the factor 0.437 accounts both for the difference in  $x_F$  and  $\sqrt{s}$  domains. It is calculated using the Schuler parametrization [17] which describes the  $\sqrt{s}$ -dependence of the  $J/\psi$  cross section<sup>3</sup>. The factor 2 limits the  $\cos(\theta_{CS})$  values to the domain  $|\cos(\theta_{CS})| < 0.5$ . The rescaled NA3  $J/\psi$  cross section thus obtained is  $4.2 \pm 1.1$  nb and agrees, within the big uncertainties, with the value  $5.5 \pm 0.4$  nb found in this paper.

## 6 Conclusion

In pp and pd collisions at 450 GeV/ $c$ , we have measured  $J/\psi$ ,  $\psi'$  and Drell-Yan cross sections as well as the ratios  $B'\sigma_{\psi'}/B\sigma_\psi$  and  $B\sigma_\psi/\sigma_{DY}$  with rather good precision. Taking into account the isospin correction for Drell-Yan in pd collisions, all the cross sections are compatible for the two reactions.

## References

- [1] P. Amaudruz et al., Phys. Rev. Lett. 66 (1991) 2712.
- [2] A. Baldit et al., NA51 Collaboration, Phys. Lett. B 332 (1994) 244.
- [3] B. Espagnon, Ph. D. Thesis, Clermont-Ferrand (1995).
- [4] L. Anderson et al., NA10 Collaboration, N.I.M. 223 (1984) 26.

---

<sup>3</sup>The Schuler parametrization is given by  $\sigma(\sqrt{s}) = \sigma_0 \times (1 - M_\psi/\sqrt{s})^{12.0 \pm 0.9}$  and the  $x_F$ -dependence is given by  $1/(1 - x_F^2) \exp(-3.12 [\ln((1 + x_F)/(1 - x_F))]^2)$ .

- [5] S. Papillon, Ph. D. Thesis, Orsay (1991); S. Constantinescu et al., IPNO-DRE 86-01 (1986).
- [6] A. D. Martin et al., Phys. Rev. D51 (1995) 4756.
- [7] H. Plochow-Besch, Comp. Phys. Comm. 75 (1993) 396.
- [8] C. Grosso-Pilcher and M.J. Sochet, Ann. Rev. Nucl. Part. Sci. 36 (1986) 1.
- [9] K. Freudenreich, Intern. Journ. of Mod. Phys. A5 (1990) 3643.
- [10] F. Fleuret, Ph. D. Thesis, Paris (1997).
- [11] R. M. Barnett et al., Phys. Rev. D54 (1996) 1.
- [12] M.C. Abreu et al., NA38 Collaboration, Nucl. Phys. A 566 (1994) 77c.
- [13] D.M. Alde et al., E772 Collaboration, Phys. Rev. Lett. 66 (1991) 133.
- [14] A.G. Clark et al., R702 Collaboration, Nucl. Phys. B 142 (1978) 29; Antoniazzi et al., E705 Collaboration, Phys. Rev. D 46 (1992) 4826; H.D. Snyder et al., E444 Collaboration, Phys. Rev. Lett. 42 (1979) 944.
- [15] W.M. Geist, Nucl. Phys. A 525 (1991) 149c.
- [16] J. Badier et al., NA3 Collaboration, Z. Phys. C 20 (1983) 101.
- [17] G.A. Schuler, CERN-TH/94-7170.